



Isotopic yields from supernova light curves

Astrophysics and Nuclear Structure

Hirscheegg, January 29, 2013

Ivo Rolf Seitenzahl

Institut für Theoretische Physik und Astrophysik

Julius-Maximilians-Universität Würzburg

Main collaborators for this work: F. Ciaraldi-Schoolmann, M. Fink,
W. Hillebrandt, M. Kromer, R. Pakmor, F. Röpke, A. Ruiter, S. Sim,
S. Taubenberger



Emmy Noether
Research Group

SN Ia

Part I: Explosive nucleosynthesis and radionuclides

- ▶ Explosive nucleosynthesis
- ▶ Radioactive decay
- ▶ Important radionuclides for supernova light curves

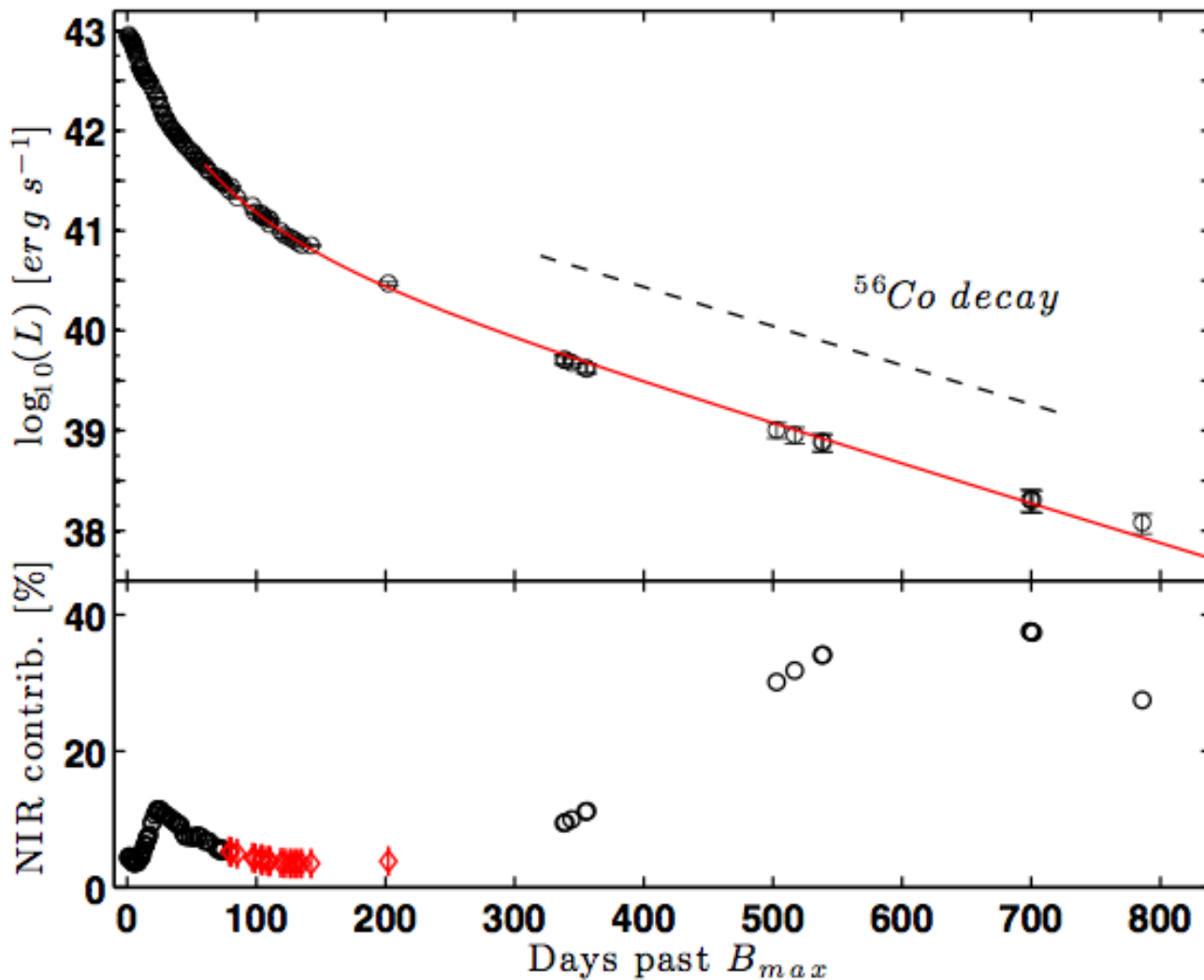
Part II: Late time supernova light curves – diagnostic power

- ▶ Bolometric supernova light curves in the lepton dominated phase
- ▶ High central density (Chandrasehkar-mass) vs low central density (violent merger) models

Type Ia SN 2003hv

After ~ 200 d, bolometric light curve (that is, luminosity integrated over UVOIR wavelengths as a function of time) is following ^{56}Co half life.

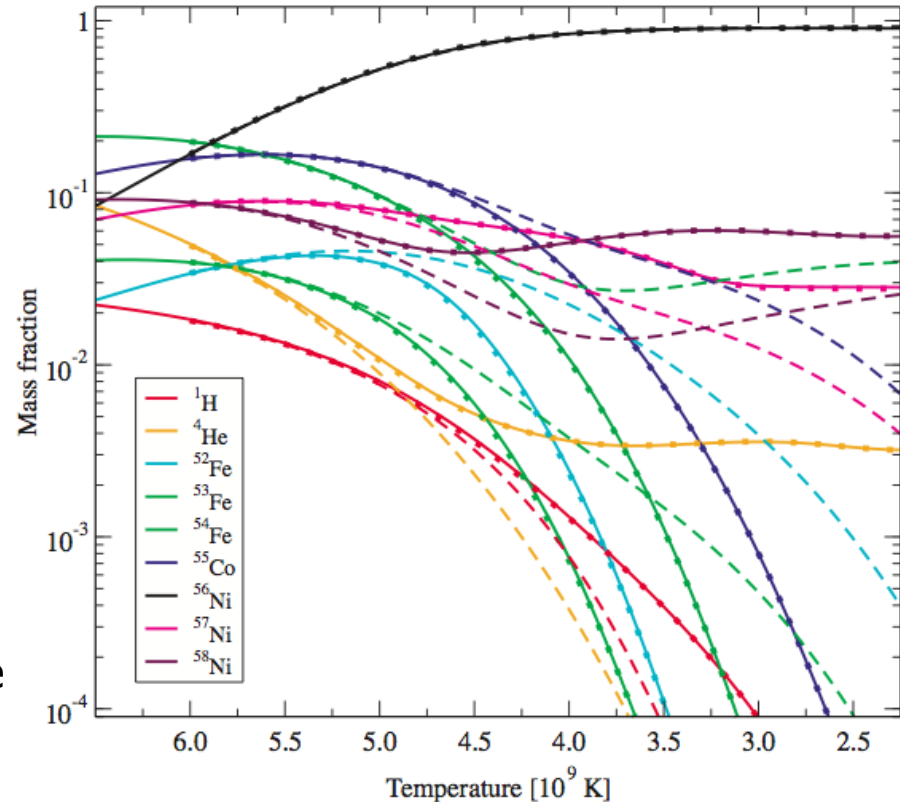
Departure at ~ 800 d is due to nuclear structure of ^{57}Fe !



(Leloudas et al, 2009, A&A, 505, 265)

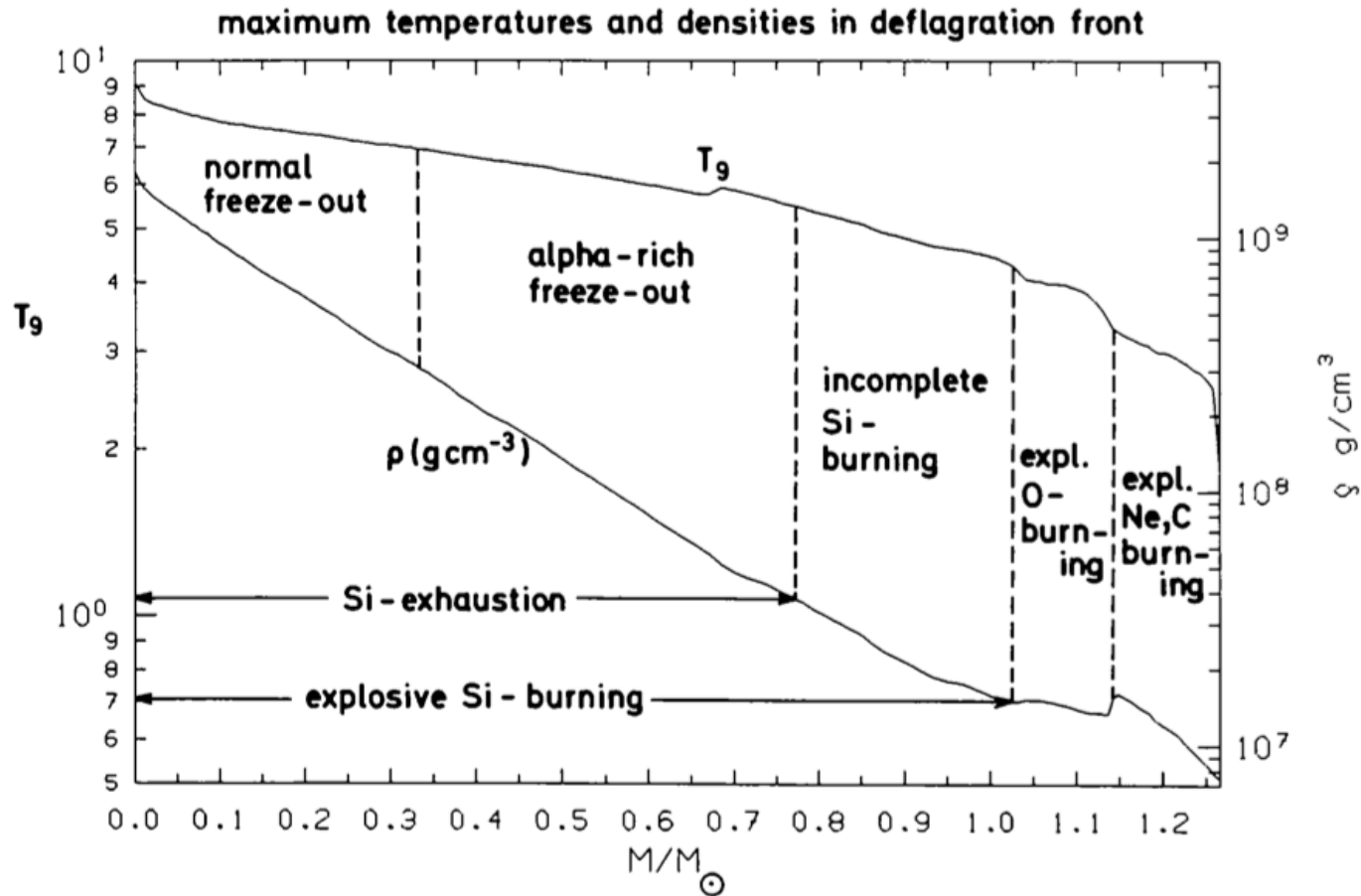
Explosive nucleosynthesis

- ▶ Thermonuclear fusion in supernovae does not proceed under hydrostatic conditions, rather in a rapidly expanding medium.
- ▶ Often temperatures reached are high enough that reaction rates are so fast that nuclear statistical equilibrium (NSE) is reached. $Y_e \sim 0.5$
- ▶ In NSE, all nuclear reactions are in detailed balance, and the equilibrium mass fractions are determined by minimizing the Helmholtz free energy $F=(U-Q)-TS$.
 - High entropy environments are dominated by light particles (such as $p, n, {}^4\text{He}$).
 - Low entropy environments are dominated by nuclei with the highest binding energy for the given neutron excess (here: Fe-group).



Mass fractions during expansion as a function of decreasing temperature. NSE values are dashed. Solid lines are reaction network calculations. Freeze-out occurs at low temperature, when nuclear reactions are too slow to keep the abundance in equilibrium for the rapidly changing thermodynamic conditions.

Example: nucleosynthesis conditions in SNe Ia



Thielemann et al. 1986

Normal freeze-out from NSE:

- ▶ Lower entropy, higher densities $> 3e8 \text{ g cm}^{-3}$
- ▶ Low light particle fraction during freeze-out
- ▶ ^{55}Co survives

Alpha-rich freeze-out from NSE

- ▶ Higher entropy, lower densities $< 3e8 \text{ g cm}^{-3}$
- ▶ High light particle fraction during freeze-out
- ▶ ^{55}Co destroyed by $^{55}\text{Co}(p,\gamma)^{56}\text{Ni}$

Nuclear Decay

Positron (electron) emission:

- ▶ Proton in the nucleus decays into a neutron, positron, and electron neutrino. The **positron** and neutrino are ejected. Only possible if $|\Delta E_{\text{bind}}| > m_n - m_p + m_e = 1.8 \text{ MeV}$.
- ▶ Nuclei that have an open positron channel always also have an admixture of electron capture, unless completely ionized, since here $|\Delta E_{\text{bind}}| > m_n - m_p - m_e = 0.8 \text{ MeV}$.
- ▶ For neutron rich nuclei, neutron in the nucleus decays into proton, **electron**, and electron anti-neutrino (positron capture generally not important here).

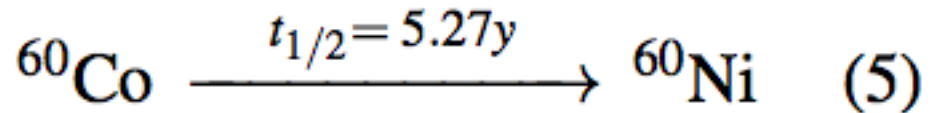
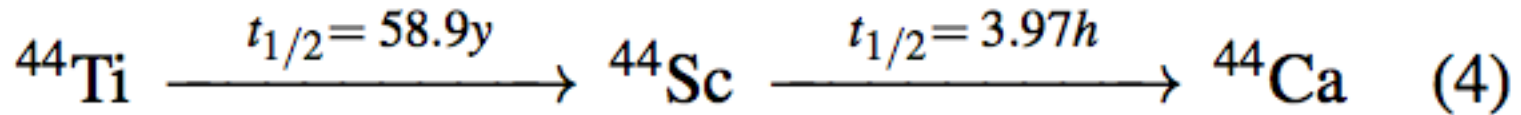
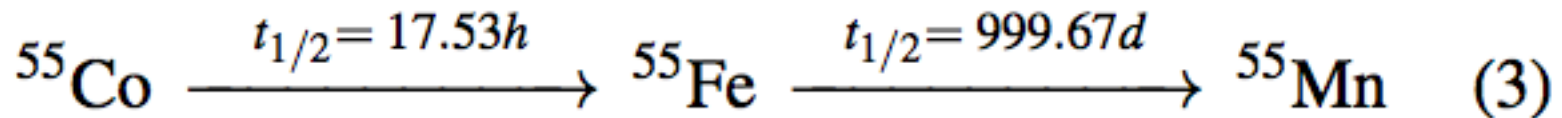
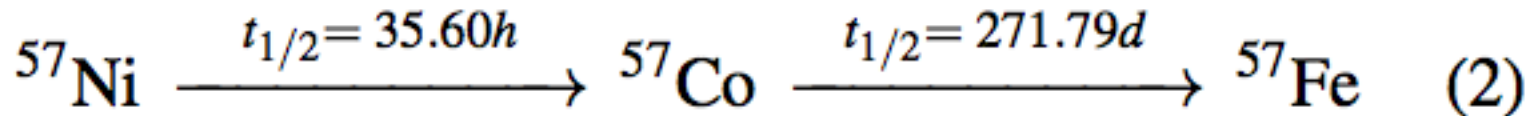
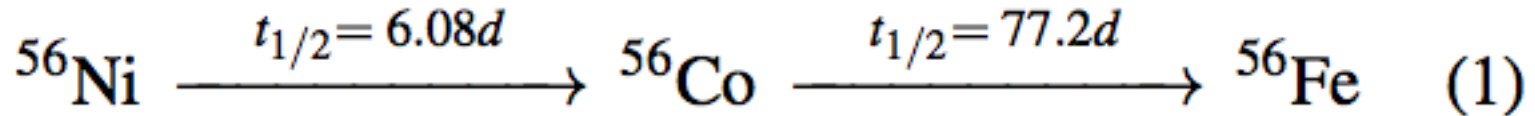
Orbital (usually K/L-shell) electron capture by a proton in the nucleus:

- ▶ Daughter has a hole in the inner atomic electron structure.
 - ▶ Hole is generally filled by higher lying electrons transitioning to lower lying levels emitting **X-rays** in the cascade.
 - ▶ Energy difference and quantum numbers can also be transferred to an outer electron, which is ejected: **Auger electrons**.

In both cases the transition can be either to an excited state or the ground state:

- ▶ If the transition is to an excited state, generally a cascade of **gamma rays** is emitted.
- ▶ Energy difference of nuclear states and quantum numbers can also be transferred to an (inner) atomic electron, which is ejected : **Internal conversion electrons**.

Relevant nuclear decay chains



- ▶ ${}^{56}\text{Ni}$ is produced most abundantly by far → most important decay chain
- ▶ In 1/5 decays ${}^{56}\text{Co}$ emits a **positron** → important at late times
- ▶ ${}^{57}\text{Co}$ decay also produces **electrons** → important at late times
- ▶ ${}^{55}\text{Co}$ decay chain generally ignored since it's 100% electron capture to the ground-state
- ▶ ${}^{55}\text{Fe}$ decay produces **electrons** → important at late times

(importance of electron channels pointed out by: Seitenzahl, Taubenberger, Sim et al. 2009, MNRAS 400, 531)

⁵⁷Co

| ⁵⁵ Cu 27 MS ε: 100.00% εp: 15.0% | ⁵⁶ Cu 93 MS ε: 100.00% εp: 0.40% | ⁵⁷ Cu 196.3 MS ε: 100.00% | ⁵⁸ Cu 3.204 S ε: 100.00% | ⁵⁹ Cu 81.5 S ε: 100.00% | ⁶⁰ Cu 23.7 M ε: 100.00% | ⁶¹ Cu 3.333 H ε: 100.00% | ⁶² Cu 9.673 M ε: 100.00% | ⁶³ Cu STABLE 69.15% | | | | | | | | | | | | |
|--|--|---|--|--|--|---|---|--|------------------|--|--|--|----------|----|------------------|-------------|-----|------|----------|--------------|
| ⁵⁴ Ni 104 MS ε: 100.00% | ⁵⁵ Ni 204.7 MS ε: 100.00% | ⁵⁶ Ni 6.075 D ε: 100.00% | ⁵⁷ Ni 35.60 H ε: 100.00% | ⁵⁸ Ni STABLE 68.077% | ⁵⁹ Ni 7.6E+4 Y ε: 100.00% | ⁶⁰ Ni STABLE 26.223% | ⁶¹ Ni STABLE 1.1399% | ⁶² Ni STABLE 3.6346% | | | | | | | | | | | | |
| ⁵³ Co 240 MS ε: 100.00% | ⁵⁴ Co 193.28 MS ε: 100.00% | ⁵⁵ Co 17.53 H ε: 100.00% | ⁵⁶ Co 77.236 D ε: 100.00% | ⁵⁷ Co 271.74 D ε: 100.00% | ⁵⁸ Co | ⁵⁹ Co | ⁶⁰ Co | ⁶¹ Co 1.650 H ε: 100.00% | | | | | | | | | | | | |
| | | | | | <table border="1"> <thead> <tr> <th colspan="4">⁵⁷Co</th> </tr> <tr> <th>E(level)</th> <th>Jπ</th> <th>T_{1/2}</th> <th>Decay Modes</th> </tr> </thead> <tbody> <tr> <td>0.0</td> <td>7/2-</td> <td>271.74 d</td> <td>ε : 100.00 %</td> </tr> </tbody> </table> | | | | ⁵⁷ Co | | | | E(level) | Jπ | T _{1/2} | Decay Modes | 0.0 | 7/2- | 271.74 d | ε : 100.00 % |
| ⁵⁷ Co | | | | | | | | | | | | | | | | | | | | |
| E(level) | Jπ | T _{1/2} | Decay Modes | | | | | | | | | | | | | | | | | |
| 0.0 | 7/2- | 271.74 d | ε : 100.00 % | | | | | | | | | | | | | | | | | |
| ⁵² Fe 8.275 H ε: 100.00% | ⁵³ Fe 8.51 M ε: 100.00% | ⁵⁴ Fe STABLE 5.845% | ⁵⁵ Fe 2.744 Y ε: 100.00% | ⁵⁶ Fe STABLE 91.754% | ⁵⁷ Fe STABLE 2.119% | ⁵⁸ Fe STABLE 0.282% | ⁵⁹ Fe 44.495 D β-: 100.00% | ⁶⁰ Fe 2.62E+6 Y β-: 100.00% | | | | | | | | | | | | |
| ⁵¹ Mn 46.2 M ε: 100.00% | ⁵² Mn 5.591 D ε: 100.00% | ⁵³ Mn 3.74E+6 Y ε: 100.00% | ⁵⁴ Mn 312.12 D ε: 100.00% β- < 2.9E-4% | ⁵⁵ Mn STABLE 100% | ⁵⁶ Mn 2.5789 H β-: 100.00% | ⁵⁷ Mn 85.4 S β-: 100.00% | ⁵⁸ Mn 3.0 S β-: 100.00% | ⁵⁹ Mn 4.59 S β-: 100.00% | | | | | | | | | | | | |

^{57}Co Gamma and X-rays

Gamma and X-ray radiation:

| | Energy (keV) | Intensity (%) | Dose (MeV/Bq-s) |
|----------------|-----------------|------------------|----------------------|
| XR 1 | 0.7 | 1.52 % 15 | 1.06E-5 11 |
| XR $k\alpha_2$ | 6.391 | 16.6 % 9 | 0.00106 5 |
| XR $k\alpha_1$ | 6.404 | 32.9 % 15 | 0.00211 10 |
| XR $k\beta_1$ | 7.058 | 3.91 % 19 | 2.76E-4 13 |
| XR $k\beta_3$ | 7.058 | 2.00 % 10 | 1.41E-4 7 |
| —▶ | 14.4129 6 | 9.16 % 15 | 0.001320 22 |
| —▶ | 122.06065 12 | 85.60 % 17 | 0.10448 21 |
| —▶ | 136.47356 29 | 10.68 % 8 | 0.01458 11 |
| | 230.4 4 | 4E-4 % 4 | 9E-7 9 |
| | 339.69 21 | 0.0037 % 3 | 1.26E-5 10 |
| | 352.33 21 | 0.0030 % 3 | 1.06E-5 11 |
| | 366.8 3 | 0.0012 % 3 | 4.4E-6 11 |
| | 570.09 20 | 0.0158 % 10 | 9.0E-5 6 |
| | 692.41 7 | 0.149 % 10 | 0.00103 7 |
| | 706.54 22 | 0.0050 % 5 | 3.5E-5 4 |

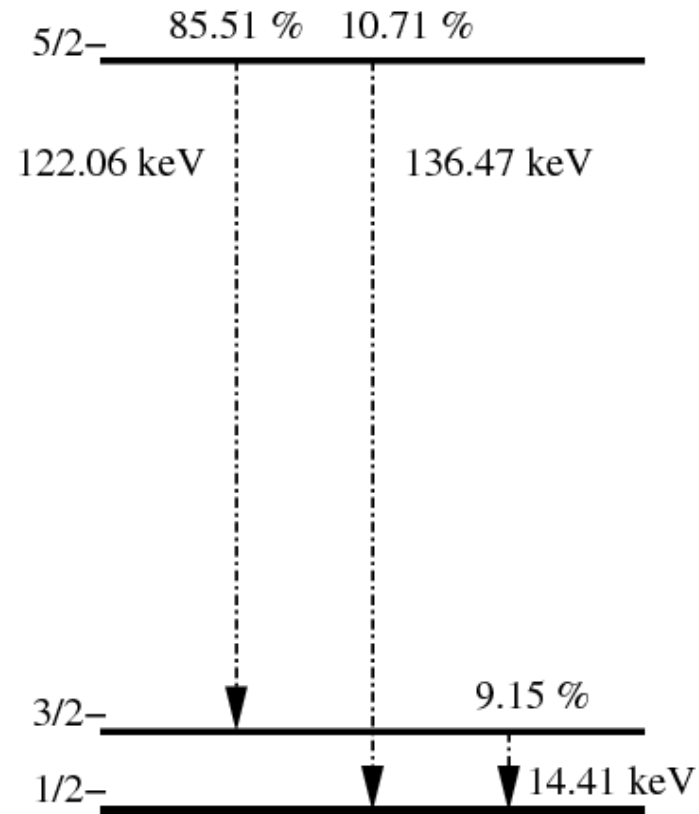
^{57}Co electrons

- ▶ Internal conversion electrons are significant due to a fortuitously low lying $3/2^-$ state in the daughter ^{57}Fe
- ▶ Combined with Auger electrons about 18 keV per decay, which can compete with the positron of ^{56}Co decay due to the longer half life of ^{57}Co

Electrons:

| | Energy (keV) | Intensity (%) | Dose (MeV/Bq-s) |
|-----------|--------------|---------------|-----------------|
| ▶ Auger L | 0.67 | 251 % 4 | 0.001684 24 |
| ▶ Auger K | 5.62 | 105.1 % 17 | 0.00591 10 |
| ▶ CE K | 7.3009 11 | 71.1 % 24 | 0.00519 18 |
| ▶ CE L | 13.5668 7 | 7.4 % 3 | 1.00E-3 3 |
| ▶ CE K | 114.9487 9 | 1.83 % 10 | 0.00211 12 |
| ▶ CE L | 121.2146 4 | 0.192 % 17 | 2.32E-4 21 |
| ▶ CE K | 129.3616 9 | 1.30 % 14 | 0.00169 18 |

No positrons!
Decay energy too low!



Level scheme and intensities for ^{57}Fe

^{55}Fe

| ^{53}Ni 55.2 MS ϵ : 100.00% ϵ_p : 23.40% | ^{54}Ni 104 MS ϵ : 100.00% | ^{55}Ni 204.7 MS ϵ : 100.00% | ^{56}Ni 6.075 D ϵ : 100.00% | ^{57}Ni 35.60 H ϵ : 100.00% | ^{58}Ni STABLE 68.077% | ^{59}Ni 7.6E+4 Y ϵ : 100.00% | ^{60}Ni STABLE 26.223% | ^{61}Ni STABLE 1.1399% | | | | | | | | | | | | |
|--|--|---|---|---|--|--|---|--|--|--|--|----------|---------|------------|-------------|-----|------|-----------|-----------------------|---|
| ^{52}Co 115 MS ϵ : 100.00% | ^{53}Co 240 MS ϵ : 100.00% | ^{54}Co 193.28 MS ϵ : 100.00% | ^{55}Co 17.53 H ϵ : 100.00% | ^{56}Co 77.236 D ϵ : 100.00% | ^{57}Co 271.74 D ϵ : 100.00% | ^{58}Co 70.86 D ϵ : 100.00% | ^{59}Co STABLE 100% | ^{60}Co 1925.28 D β^- : 100.00% | | | | | | | | | | | | |
| ^{51}Fe 305 MS ϵ : 100.00% | ^{52}Fe 8.275 H ϵ : 100.00% | ^{53}Fe 8.51 M ϵ : 100.00% | ^{54}Fe STABLE 5.845% | ^{55}Fe 2.744 Y ϵ : 100.00% | <table border="1"> <thead> <tr> <th colspan="4">^{55}Fe</th> </tr> <tr> <th>E(level)</th> <th>Jπ</th> <th>T$_{1/2}$</th> <th>Decay Modes</th> </tr> </thead> <tbody> <tr> <td>0.0</td> <td>3/2-</td> <td>2.744 y 9</td> <td>ϵ: 100.00 %</td> </tr> </tbody> </table> | | | ^{55}Fe | | | | E(level) | J π | T $_{1/2}$ | Decay Modes | 0.0 | 3/2- | 2.744 y 9 | ϵ : 100.00 % | ^{59}Fe 44.495 D β^- : 100.00% |
| ^{55}Fe | | | | | | | | | | | | | | | | | | | | |
| E(level) | J π | T $_{1/2}$ | Decay Modes | | | | | | | | | | | | | | | | | |
| 0.0 | 3/2- | 2.744 y 9 | ϵ : 100.00 % | | | | | | | | | | | | | | | | | |
| ^{50}Mn 283.19 MS ϵ : 100.00% | ^{51}Mn 46.2 M ϵ : 100.00% | ^{52}Mn 5.591 D ϵ : 100.00% | ^{53}Mn 3.74E+6 Y ϵ : 100.00% | ^{54}Mn 312.12 D ϵ : 100.00% β^- : < 2.9E-4% | ^{55}Mn STABLE 100% | ^{56}Mn 2.5789 H β^- : 100.00% | ^{57}Mn 85.4 S β^- : 100.00% | ^{58}Mn 3.0 S β^- : 100.00% | | | | | | | | | | | | |
| ^{49}Cr 42.3 M ϵ : 100.00% | ^{50}Cr >1.3E+18 Y 4.345% 2 ϵ | ^{51}Cr 27.7025 D ϵ : 100.00% | ^{52}Cr STABLE 83.789% | ^{53}Cr STABLE 9.501% | ^{54}Cr STABLE 2.365% | ^{55}Cr 3.497 M β^- : 100.00% | ^{56}Cr 5.94 M β^- : 100.00% | ^{57}Cr 21.1 S β^- : 100.00% | | | | | | | | | | | | |

^{55}Fe decay radiation

Very low decay energy. Almost 100% GS to GS transition!

Essentially no gamma rays! But:

Electrons:

| | Energy (keV) | Intensity (%) | Dose (MeV/Bq-s) |
|-----------|-----------------|------------------|----------------------|
| → Auger L | 0.61 | 139.9 % 14 | 8.53E-4 8 |
| → Auger K | 5.19 | 60.1 % 8 | 0.00312 4 |

Gamma and X-ray radiation:

| | Energy (keV) | Intensity (%) | Dose (MeV/Bq-s) | |
|---|-----------------|------------------|----------------------|------------|
| | XR 1 | 0.64 | 0.66 % 10 | 4.2E-6 6 |
| → | XR $k\alpha_2$ | 5.888 | 8.2 % 4 | 4.85E-4 21 |
| → | XR $k\alpha_1$ | 5.899 | 16.2 % 7 | 9.6E-4 4 |
| | XR $k\beta_1$ | 6.49 | 1.89 % 9 | 1.23E-4 6 |
| | XR $k\beta_3$ | 6.49 | 0.96 % 5 | 6.3E-5 3 |
| | | 126.0 1 | 1.280E-7 % 20 | 1.61E-10 3 |

Bolometric light curves

Basics:

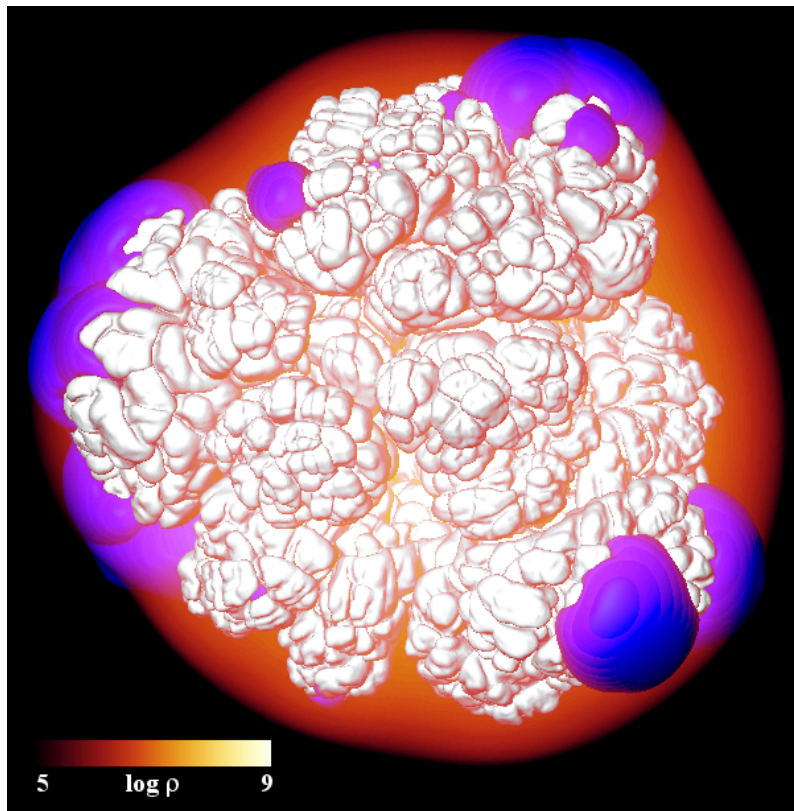
- ▶ Usually, bolometric light curves are reconstructed from UVOIR data.
- ▶ IR bands are progressively more important at late times as the wavelength of the peak emission shifts into further and further into the red → infrared catastrophe
- ▶ Unfortunately, only very few IR observations exist, especially at late times
- ▶ Column density and hence opacity to gamma-rays decreases as t^{-2}

Models:

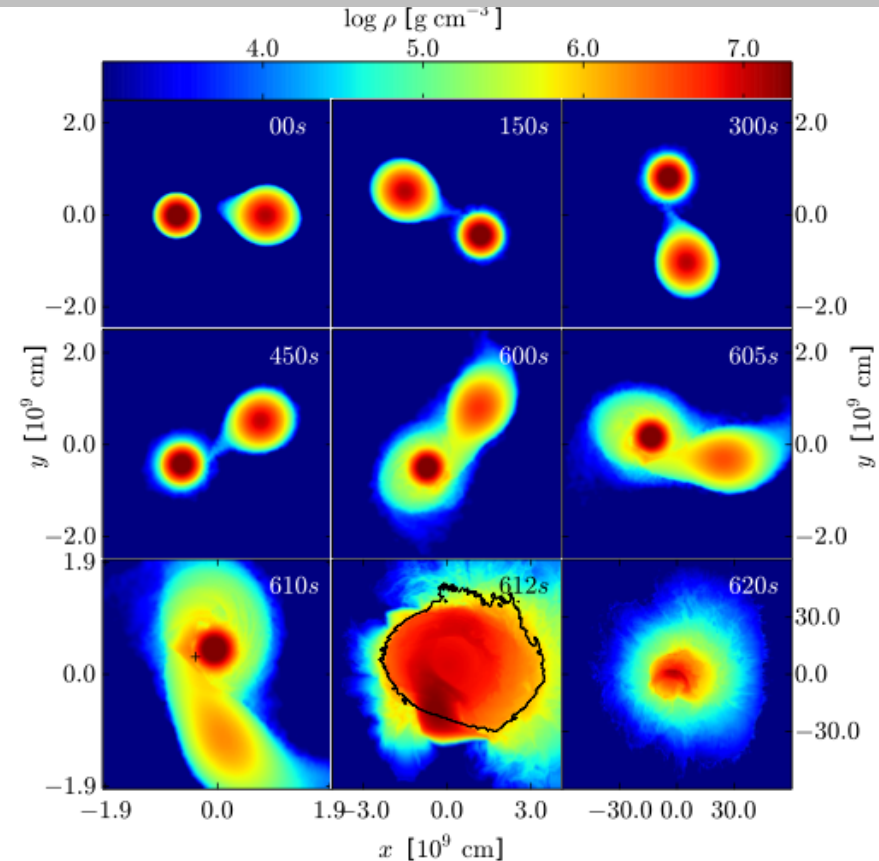
- ▶ Detailed models treat radiative transfer of photons
 - ▶ Abundances and density/velocity profile needed for source terms, opacities, and time evolution
 - ▶ Processes include Compton scattering, pair-production, photoelectric-absorption (bound-free), collisional processes, Bremsstrahlung
- ▶ Local and complete deposition of positron kinetic energy is usually assumed
 - ▶ Escape fraction of positrons at late times remains an open question
- ▶ At late times, when most gamma-rays escape and leptons dominate the energy input, the bolometric light curve falls with the half life of the dominant leptonic channel

M_{ch} delayed detonation vs. violent merger

| | delayed detonation M_{ch} WD | violent merger ($1.1+0.9 M_{\odot}$ WD) |
|---|---------------------------------------|--|
| ^{56}Ni mass [M_{\odot}] | 0.604 | 0.616 |
| mass of ^{57}Ni and ^{57}Co [M_{\odot}] | 1.88×10^{-2} | 1.49×10^{-2} |
| mass of ^{55}Fe and ^{55}Co [M_{\odot}] | 1.33×10^{-2} | 3.73×10^{-3} |



(Seitenzahl, Ciaraldi-Schoolmann, Röpke et al. 2013, MNRAS 429, 1156)



Pakmor et al. (2012) ApJ 747, 10

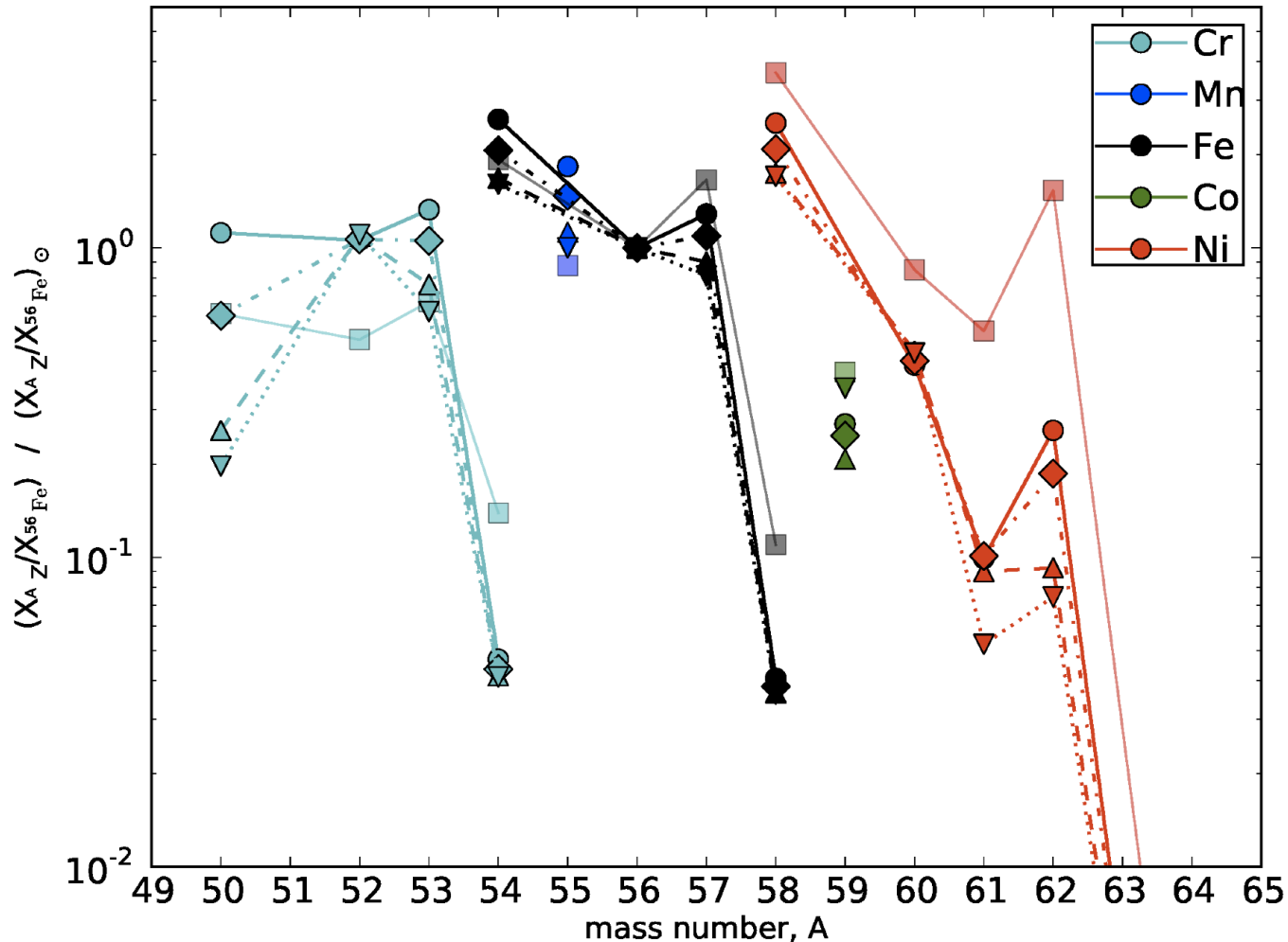
New 3D delayed detonation SNe Ia yield tables

Table 2. Asymptotic nucleosynthetic yields (in solar masses) of stable nuclides.

| | N1 | N3 | N5 | N10 | N20 | N40 | N100H | N100 | N100L | N150 | N200 | N300C | N1600 | N1600C | N100_Z0.5 | N100_Z0.1 | N100_Z0.01 |
|------------------|----------|----------|----------|----------|----------|----------|----------|----------|----------|----------|----------|----------|----------|----------|-----------|-----------|------------|
| ¹² C | 2.61E-03 | 9.90E-03 | 9.05E-03 | 4.43E-03 | 9.20E-03 | 3.90E-03 | 3.87E-03 | 3.04E-03 | 3.85E-03 | 1.72E-02 | 1.21E-02 | 8.86E-03 | 1.06E-02 | 1.68E-02 | 3.10e-03 | 3.15e-03 | 3.16e-03 |
| ¹³ C | 1.84E-08 | 6.15E-08 | 5.05E-08 | 2.57E-08 | 4.52E-08 | 2.18E-08 | 2.28E-08 | 1.74E-08 | 2.17E-08 | 1.00E-07 | 6.57E-08 | 4.95E-08 | 5.57E-08 | 8.44E-08 | 8.47e-09 | 1.91e-09 | 2.72e-10 |
| ¹⁴ N | 2.92E-06 | 9.93E-06 | 8.46E-06 | 3.85E-06 | 8.34E-06 | 4.30E-06 | 4.25E-06 | 3.21E-06 | 3.98E-06 | 1.84E-05 | 1.33E-05 | 9.16E-06 | 1.04E-05 | 1.88E-05 | 1.80e-06 | 4.71e-07 | 7.22e-08 |
| ¹⁵ N | 3.36E-09 | 1.22E-08 | 1.03E-08 | 4.47E-09 | 1.03E-08 | 5.16E-09 | 5.24E-09 | 3.67E-09 | 4.66E-09 | 2.29E-08 | 1.71E-08 | 1.14E-08 | 1.29E-08 | 2.41E-08 | 2.07e-09 | 2.98e-09 | 8.73e-08 |
| ¹⁶ O | 2.63E-02 | 4.74E-02 | 5.63E-02 | 5.16E-02 | 9.04E-02 | 9.89E-02 | 7.30E-02 | 1.01E-01 | 1.24E-01 | 1.24E-01 | 1.96E-01 | 1.21E-01 | 1.91E-01 | 2.72E-01 | 9.87e-02 | 9.64e-02 | 9.47e-02 |
| ¹⁷ O | 3.96E-07 | 1.37E-06 | 1.16E-06 | 5.34E-07 | 1.12E-06 | 5.54E-07 | 5.61E-07 | 4.13E-07 | 5.14E-07 | 2.48E-06 | 1.74E-06 | 1.22E-06 | 1.36E-06 | 2.42E-06 | 2.84e-07 | 9.32e-08 | 5.43e-09 |
| ¹⁸ O | 3.32E-09 | 1.33E-08 | 1.11E-08 | 4.54E-09 | 1.12E-08 | 5.29E-09 | 5.59E-09 | 3.53E-09 | 4.61E-09 | 2.52E-08 | 1.98E-08 | 1.25E-08 | 1.44E-08 | 2.73E-08 | 2.23e-09 | 1.21e-09 | 9.93e-10 |
| ¹⁹ F | 3.73E-11 | 1.35E-10 | 1.17E-10 | 5.05E-11 | 1.22E-10 | 6.22E-11 | 6.32E-11 | 4.39E-11 | 5.68E-11 | 2.64E-10 | 2.13E-10 | 1.36E-10 | 1.58E-10 | 2.97E-10 | 2.20e-11 | 1.48e-11 | 4.79e-11 |
| ²⁰ Ne | 1.47E-03 | 3.37E-03 | 3.75E-03 | 2.40E-03 | 5.41E-03 | 4.15E-03 | 3.66E-03 | 3.53E-03 | 4.33E-03 | 8.72E-03 | 1.15E-02 | 6.76E-03 | 9.40E-03 | 1.73E-02 | 3.60e-03 | 3.19e-03 | 3.74e-03 |
| ²¹ Ne | 3.08E-07 | 9.79E-07 | 8.81E-07 | 4.16E-07 | 9.63E-07 | 5.43E-07 | 5.20E-07 | 4.11E-07 | 5.17E-07 | 1.98E-06 | 1.68E-06 | 1.08E-06 | 1.29E-06 | 2.39E-06 | 1.97e-07 | 1.47e-08 | 6.93e-09 |
| ²² Ne | 6.40E-05 | 3.26E-04 | 2.87E-04 | 1.31E-04 | 2.58E-04 | 5.77E-05 | 7.62E-05 | 4.07E-05 | 5.51E-05 | 4.83E-04 | 2.34E-04 | 2.11E-04 | 2.32E-04 | 2.97E-04 | 1.65e-05 | 2.30e-06 | 1.71e-07 |
| ²³ Na | 2.20E-05 | 6.41E-05 | 6.09E-05 | 3.22E-05 | 7.30E-05 | 4.66E-05 | 4.25E-05 | 3.74E-05 | 4.68E-05 | 1.38E-04 | 1.38E-04 | 8.53E-05 | 1.09E-04 | 2.01E-04 | 2.63e-05 | 1.96e-05 | 1.72e-05 |
| ²⁴ Mg | 3.93E-03 | 7.13E-03 | 8.53E-03 | 7.77E-03 | 1.46E-02 | 1.54E-02 | 1.15E-02 | 1.52E-02 | 1.83E-02 | 1.93E-02 | 3.32E-02 | 1.97E-02 | 3.08E-02 | 4.61E-02 | 2.02e-02 | 2.69e-02 | 2.90e-02 |
| ²⁵ Mg | 3.35E-05 | 9.26E-05 | 8.92E-05 | 5.07E-05 | 1.11E-04 | 7.70E-05 | 6.86E-05 | 6.49E-05 | 8.02E-05 | 2.02E-04 | 2.14E-04 | 1.33E-04 | 1.75E-04 | 3.12E-04 | 3.09e-05 | 1.06e-05 | 8.99e-07 |
| ²⁶ Mg | 5.15E-05 | 1.36E-04 | 1.34E-04 | 7.55E-05 | 1.71E-04 | 1.17E-04 | 1.04E-04 | 9.66E-05 | 1.19E-04 | 3.07E-04 | 3.27E-04 | 2.01E-04 | 2.61E-04 | 4.82E-04 | 4.44e-05 | 7.36e-06 | 1.04e-06 |
| ²⁷ Al | 1.98E-04 | 3.95E-04 | 4.56E-04 | 3.71E-04 | 7.32E-04 | 7.05E-04 | 5.47E-04 | 6.74E-04 | 8.32E-04 | 1.04E-03 | 1.14E-03 | 7.68E-04 | 1.48E-03 | 2.37E-03 | 5.88e-04 | 2.68e-04 | 8.71e-05 |
| ²⁸ Si | 6.32E-02 | 8.99E-02 | 1.19E-01 | 1.38E-01 | 1.98E-01 | 2.59E-01 | 2.12E-01 | 2.84E-01 | 3.55E-01 | 2.71E-01 | 2.71E-01 | 3.19E-01 | 3.61E-01 | 3.44E-01 | 2.90e-01 | 2.94e-01 | 2.89e-01 |
| ²⁹ Si | 2.69E-04 | 4.64E-04 | 5.68E-04 | 5.17E-04 | 9.49E-04 | 1.03E-03 | 7.73E-04 | 1.03E-03 | 1.25E-03 | 1.30E-03 | 2.08E-03 | 1.29E-03 | 1.97E-03 | 2.86E-03 | 7.28e-04 | 4.30e-04 | 1.35e-04 |
| ³⁰ Si | 5.96E-04 | 1.00E-03 | 1.23E-03 | 1.18E-03 | 2.12E-03 | 2.35E-03 | 1.72E-03 | 2.36E-03 | 2.86E-03 | 2.77E-03 | 4.76E-03 | 2.87E-03 | 4.53E-03 | 6.55E-03 | 1.19e-03 | 1.44e-04 | 1.84e-05 |
| ³¹ P | 1.40E-04 | 2.28E-04 | 2.87E-04 | 2.78E-04 | 4.87E-04 | 5.60E-04 | 4.20E-04 | 5.77E-04 | 7.01E-04 | 6.59E-04 | 1.08E-03 | 6.85E-04 | 1.05E-03 | 1.47E-03 | 3.58e-04 | 1.05e-04 | 3.54e-05 |
| ³² S | 2.62E-02 | 3.70E-02 | 4.79E-02 | 5.74E-02 | 7.74E-02 | 1.01E-01 | 8.55E-02 | 1.11E-01 | 1.38E-01 | 1.07E-01 | 1.10E-01 | 1.27E-01 | 1.22E-01 | 1.03E-01 | 1.12e-01 | 1.12e-01 | 1.15e-01 |
| ³³ S | 7.51E-05 | 1.06E-04 | 1.42E-04 | 1.53E-04 | 2.43E-04 | 3.14E-04 | 2.37E-04 | 3.39E-04 | 4.21E-04 | 3.27E-04 | 5.23E-04 | 3.65E-04 | 5.47E-04 | 6.79E-04 | 2.39e-04 | 1.04e-04 | 4.57e-05 |
| ³⁴ S | 8.26E-04 | 1.16E-03 | 1.57E-03 | 1.75E-03 | 2.84E-03 | 3.73E-03 | 2.73E-03 | 4.04E-03 | 5.02E-03 | 3.68E-03 | 6.22E-03 | 4.22E-03 | 6.56E-03 | 8.06E-03 | 1.86e-03 | 2.60e-04 | 7.14e-06 |
| ³⁶ S | 8.12E-08 | 1.35E-07 | 1.65E-07 | 1.41E-07 | 2.54E-07 | 2.57E-07 | 1.87E-07 | 2.47E-07 | 3.05E-07 | 3.59E-07 | 5.42E-07 | 3.23E-07 | 4.97E-07 | 7.68E-07 | 3.86e-08 | 1.64e-09 | 1.73e-11 |
| ³⁵ Cl | 4.29E-05 | 6.20E-05 | 8.27E-05 | 8.37E-05 | 1.35E-04 | 6.77E-04 | 1.27E-04 | 1.78E-04 | 2.27E-04 | 1.89E-04 | 2.89E-04 | 2.00E-04 | 2.98E-04 | 3.84E-04 | 9.91e-05 | 2.64e-05 | 5.65e-06 |
| ³⁷ Cl | 7.32E-06 | 9.62E-06 | 1.34E-05 | 1.53E-05 | 2.26E-05 | 3.14E-05 | 2.44E-05 | 3.51E-05 | 4.49E-05 | 3.14E-05 | 4.66E-05 | 3.63E-05 | 5.22E-05 | 5.75E-05 | 2.27e-05 | 9.14e-06 | 3.52e-06 |
| ³⁶ Ar | 4.52E-03 | 6.36E-03 | 8.03E-03 | 9.89E-03 | 1.28E-02 | 1.61E-02 | 1.43E-02 | 1.77E-02 | 2.17E-02 | 1.76E-02 | 1.50E-02 | 2.08E-02 | 1.64E-02 | 1.23E-02 | 1.85e-02 | 1.92e-02 | 2.04e-02 |
| ³⁸ Ar | 3.77E-04 | 5.15E-04 | 7.18E-04 | 8.01E-04 | 1.25E-03 | 1.72E-03 | 1.29E-03 | 1.91E-03 | 2.48E-03 | 1.69E-03 | 2.69E-03 | 1.96E-03 | 2.98E-03 | 3.42E-03 | 8.31e-04 | 1.19e-04 | 5.40e-06 |
| ⁴⁰ Ar | 1.68E-09 | 2.45E-09 | 3.11E-09 | 2.90E-09 | 4.79E-09 | 5.27E-09 | 3.81E-09 | 5.21E-09 | 6.60E-09 | 6.64E-09 | 1.04E-08 | 6.29E-09 | 9.87E-09 | 1.48E-08 | 4.66e-10 | 9.87e-12 | 5.11e-14 |
| ³⁹ K | 2.26E-05 | 2.98E-05 | 4.22E-05 | 4.65E-05 | 6.80E-05 | 9.52E-05 | 7.40E-05 | 1.07E-04 | 1.39E-04 | 9.53E-05 | 1.42E-04 | 1.10E-04 | 1.60E-04 | 1.75E-04 | 6.25e-05 | 1.89e-05 | 3.57e-06 |
| ⁴¹ K | 1.29E-06 | 1.63E-06 | 2.30E-06 | 2.66E-06 | 3.80E-06 | 5.38E-06 | 4.22E-06 | 6.08E-06 | 7.87E-06 | 5.36E-06 | 7.81E-06 | 6.21E-06 | 8.93E-06 | 9.65E-06 | 3.85e-06 | 1.42e-06 | 4.92e-07 |
| ⁴⁰ Ca | 4.05E-03 | 5.74E-03 | 7.09E-03 | 8.82E-03 | 1.13E-02 | 1.35E-02 | 1.24E-02 | 1.47E-02 | 1.75E-02 | 1.50E-02 | 1.07E-02 | 1.78E-02 | 1.10E-02 | 7.50E-03 | 1.57e-02 | 1.66e-02 | 1.77e-02 |

Metallicity dependent yields for 3D SNe Ia

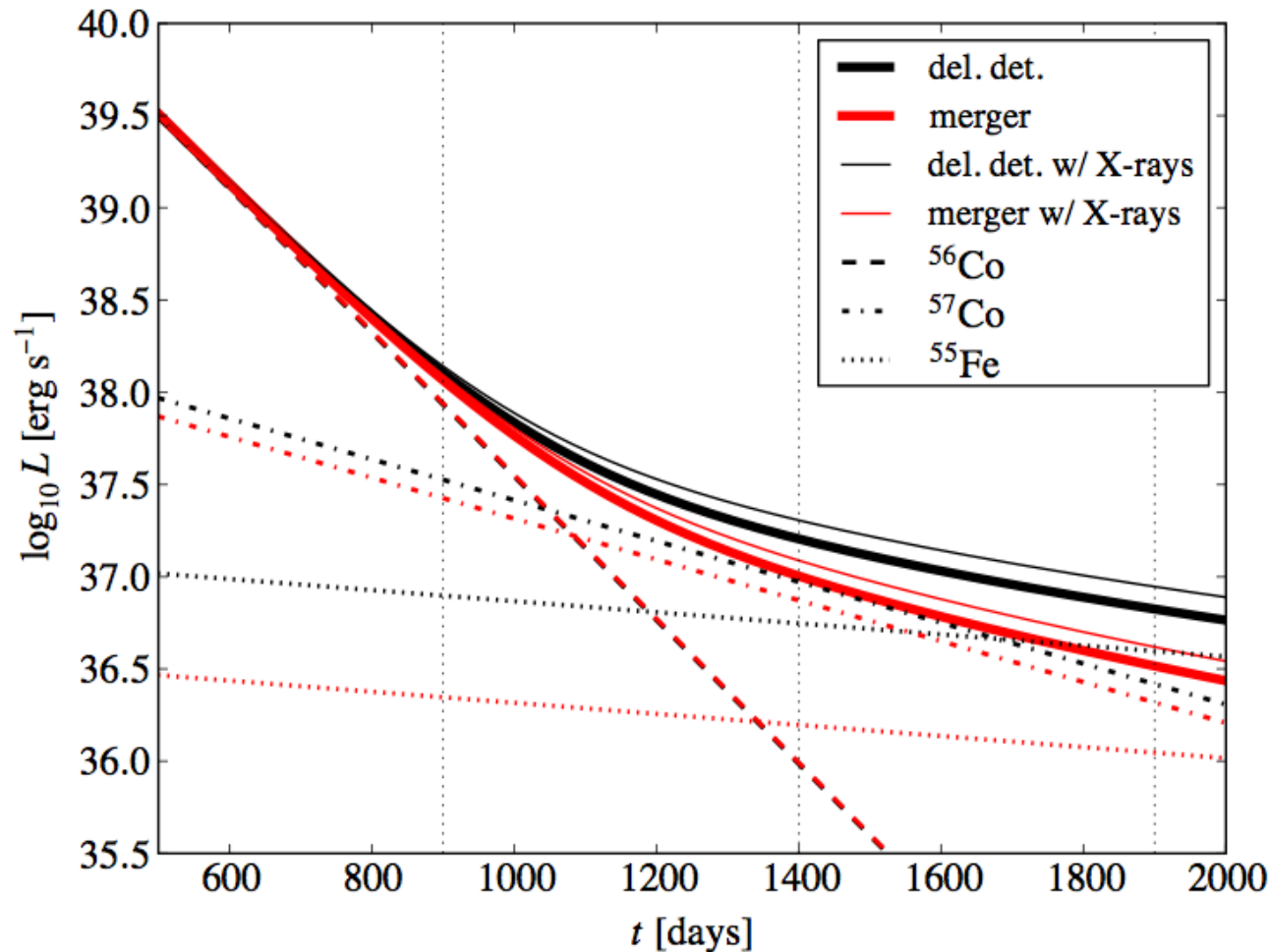
Compared to W7 (squares, Maeda 2010), 3D delayed-detonation models produce (normalized to ^{56}Fe) different yield pattern in the Fe-peak, i.e. more Mn, less Co and Ni. Coupling different SN Ia yields to chemical evolution are one possible way to distinguish models.



(Seitzzahl, Ciaraldi-Schoolmann, Röpke et al. 2013, MNRAS 429, 1156)

Possible late light curves for SN 2011fe

- ▶ Merger and delayed-detonation models produce at equal ^{56}Ni yields somewhat different ^{57}Ni and very different amounts of ^{55}Co (due to different central densities). This provides an additional, independent way to distinguish the models.



(Röpke, Kromer, Seitenzahl et al. 2011, ApJL, 750, 19)

Conclusions

- ▶ Nuclear structure has important consequences for SNe Ia, luckily (or unfortunately, depending on your point of view) the important nuclei are near the valley of stability and the relevant properties are experimentally well known.
- ▶ Electrons (internal conversion and Auger) produced in radioactive decay can be important or even dominant heat source for late phases of SNe Ia.
- ▶ Late time bolometric light curves are sensitive to isotopic production ratios of some radionuclides, which can be an independent diagnostic tool (in addition to e.g. spectral analysis).
- ▶ Future observations of late time SN light curves (e.g. SN 2011fe) hold promise of constraining central density of underlying supernova explosion, thus independently constraining explosion scenario.